

Formation of quantum dots in twofold cleaved edge overgrowth

M. Grundmann* and D. Bimberg

Institut für Festkörperphysik, Technische Universität Berlin, Hardenbergstraße 36, D-10623 Berlin, Germany

(Received 14 May 1996)

The formation of quantum dots at the juncture of three quantum-well planes, which can be fabricated with two-fold cleaved edge overgrowth, is predicted. The localization energy of the exciton ground state with respect to the connected quantum wires can exceed 10 meV for the GaAs/Al_xGa_{1-x}As system. [S0163-1829(96)05040-0]

Cleaved edge overgrowth (CEO) (Ref. 1) has been used recently to fabricate electronic *T*-shaped quantum wires (*T*-QWR), which develop at the juncture of two quantum well (QWL) planes [Figs. 1(a) and 1(b)]. The high perfection with which the quantum wells can be grown makes this system attractive for studying intrinsic effects due to localization and size quantization of carriers. Lasing at low temperature² and localization of excitonic wave functions³ have been demonstrated for such structures. In this paper we predict that the juncture of three QWL planes, as could be fabricated with twofold CEO, acts as an electronic quantum dot (QD) for electrons and holes. GaAs/Al_xGa_{1-x}As is used as a model material system for the calculations.

In Fig. 1(c) it is shown how a second cleave and overgrowth of the (110) plane creates a juncture of three QWL planes. If the initial superlattice [Fig. 1(a)] contains *N* quantum-well layers, *N* quantum dots are produced. This is not a high total number, but the perfection with which these quantum dots can be potentially made might make this system useful and interesting to perform fundamental studies of well isolated or controllably coupled quantum dots. In this paper we will discuss isolated dots only.

For the numerical solution of the three QWL system we use a finite-difference scheme with 65×65×65 voxels, and solve the three-dimensional effective-mass Schrödinger equation with laterally varying mass.⁴ The material parameters used for Al_xGa_{1-x}As, *x*≤0.4 are⁵ $E_{\text{gap}}=1.519+x \times 1.249$ eV for the bandgap, $m_e^*=0.0665+x \times 0.0575$ for the electron effective mass, $m_{\text{hh}}^*=0.45+x \times 0.05$ for the heavy hole effective mass and a conduction-band discontinuity of 65%. For AlAs we use conduction- and valence-band offsets of 1036 and 558 meV, respectively. These values are identical to those used in Ref. 3 for the simulation of CEO quantum wires. Since the electrons carry the main effect, we simplified the calculation for holes by using an isotropic mass as given above. A more detailed calculation in the framework of *kp* theory, as reported for *T*-QWR's,⁶ would also be desirable for the three-dimensional problem, but is a subject of future investigation at the moment.

As relative static dielectric constant we use the (low temperature) GaAs value $\epsilon_r=12.5$ for all parts of the structure. Image charge effects are not taken rigorously into account. Due to the extension of the electrostatic electron-hole interaction into the barrier with lower dielectric constant, the exciton binding energy is increased (an increase of the exciton binding energy for GaAs/Al_{0.4}Ga_{0.6}As quantum wells by

about 10% due to image charge effects was found in Ref. 7, for AlAs barriers ($\epsilon_r=10$) even more significant corrections will arise).

The Coulomb interaction $\mathcal{H}_C = -(e^2/4\pi\epsilon_0\epsilon_r) \times (1/|\mathbf{r}_e - \mathbf{r}_h|)$ is taken into account with a variational procedure. For the two-particle wave function of the exciton $\Psi_{\text{ex}}(\mathbf{r}_e, \mathbf{r}_h)$, we take a separated trial wave function

$$\Psi_{\text{ex}}(\mathbf{r}_e, \mathbf{r}_h) = \Psi_e(\mathbf{r}_e) \cdot \Psi_h(\mathbf{r}_h). \quad (1)$$

Let Ψ_e^0 and Ψ_h^0 be the solutions of the single-particle Hamiltonians \mathcal{H}_e and \mathcal{H}_h (kinetic energy and confinement potential), and E_e^0 and E_h^0 the single-particle ground-state energies, respectively. The exciton binding energy E_X is then given in first order perturbation theory by

$$E_X^0 = -\langle \Psi_e^0 \Psi_h^0 | H_C | \Psi_e^0 \Psi_h^0 \rangle. \quad (2)$$

In order to improve the estimate for the exciton binding energy we then iteratively solve in step *n* (*n*=1, 2, ...) the electron problem in the electrostatic potential of the hole wave function Ψ_h^{n-1} resulting in a new wave function Ψ_e^n , and then the hole problem in the electrostatic potential of the

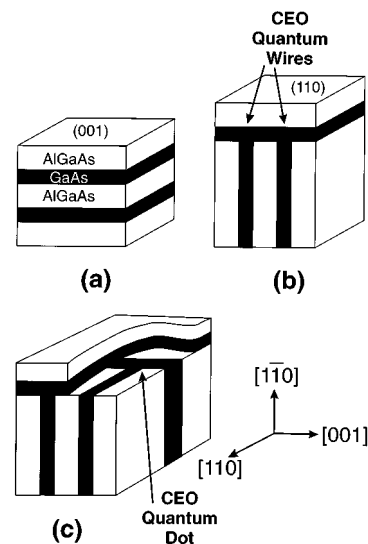


FIG. 1. Schematic representation of twofold cleaved edge overgrowth. (a) and (b) describe the standard process used for fabrication of quantum wires. In (c) a second cleave and growth on top of the (110) plane allows the fabrication of quantum dots.

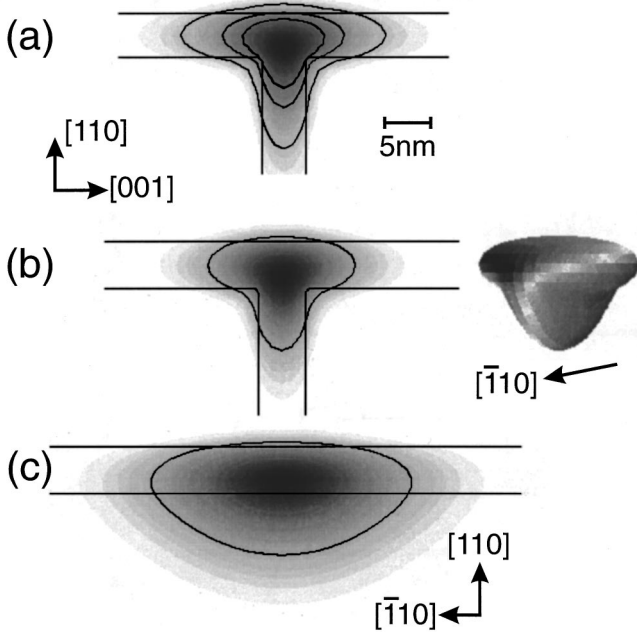


FIG. 2. (a) Single-particle electron wave-function probability (Ψ^2) in a $L_{\text{QW}}=5$ nm T -shaped $\text{GaAs}/\text{Al}_{0.35}\text{Ga}_{0.65}\text{As}$ quantum wire. Contour lines are for 90%, 70%, and 50% probability inside the line. (b) and (c) show the electron wave function (after convergence of the variational procedure, $n=5$) in the excitonic case. (c) depicts the extension along the wire, (b) shows the $(1\bar{1}0)$ cross-section plane through the center of the exciton. The perspective view (70% orbital) in (b) is rotated by 20° around the $[110]$ axis.

electron wave function Ψ_e^n resulting in a new wave function Ψ_h^n , and so on. The series of exciton binding energies

$$E_X^n = E_e^0 + E_h^0 - \langle \Psi_e^n \Psi_h^n | \mathcal{H}_e + \mathcal{H}_h + \mathcal{H}_C | \Psi_e^n \Psi_h^n \rangle \quad (3)$$

converges quickly (after about $n=4-5$ cycles for dots and wires). Graphically speaking, the electron and hole attract each other and distort the single-particle wave functions Ψ_e^0 and Ψ_h^0 as long as the energy decrease due to electrostatic energy is larger than the increase of the kinetic energy.

We generally find that electron and holes are localized at the juncture of the three planes which acts as an electronic quantum dot. There are three different barriers for the dot: the four connected QWR's, the QWL's, and the bulk barrier material. Since the QWR's have the lowest energy, the localization energy for the quantum dot E_{loc} is

$$E_{\text{loc}} = E_{\text{QD}} - E_{\text{QWR}}. \quad (4)$$

In the course of the calculation we also obtain some properties of the T -shaped quantum wire exciton, e.g., the binding energy and the wave-function extension which we will discuss first.

For our calculations we take three $\text{GaAs}/\text{Al}_{0.35}\text{Ga}_{0.65}\text{As}$ QWL's whose thicknesses L_1 , L_2 , and L_3 are taken to be identical, $L_i = L_{\text{QW}}$ (balanced structure). In Fig. 2(a) the electron wave function of a T -shaped QWR with $L_{\text{QW}}=5$ nm is shown. This plot is very similar to results in Ref. 8. If now the Coulomb interaction is included in the calculation as described above, the exciton forms and develops a finite size along the $[1\bar{1}0]$ wire direction. In Figs. 2(b) and 2(c) the

TABLE I. Extension of wave functions (in nm) for a CEO $\text{GaAs}/\text{Al}_{0.35}\text{Ga}_{0.65}\text{As}$ T -shaped quantum wire with $L_{\text{QW}}=5$ nm.

	Ψ_e^0	Ψ_e^5	Ψ_h^0	Ψ_h^5
$\sigma_{[001]}$	4.6	3.9	3.6	2.6
$\sigma_{[110]}$	3.6	3.1	2.8	2.2
$\sigma_{[1\bar{1}0]}$		7.2	∞	4.3

electron (excitonic) wave function is shown in two different cross sections. Along the QWR the extension of the wave function is now finite. In Table I the wave-function extensions in the different directions are listed for the single-particle wave function and the exciton case. The Coulomb interaction leads to a shrinking of the QWR wave function in all dimensions.

The extension of the wave function in the (110) plane [in the following (x,y) plane] can be measured by the diamagnetic shift of the recombination line in weak magnetic fields.³ The extension of the exciton wave function

$$\sqrt{\langle x^2 + y^2 \rangle} = \sqrt{\mu \left(\frac{\langle \Psi_e | x^2 + y^2 | \Psi_e \rangle}{m_e} + \frac{\langle \Psi_h | x^2 + y^2 | \Psi_h \rangle}{m_h} \right)}, \quad (5)$$

where μ is the reduced mass, is shown in Figs. 3(a) and 3(d). Our theoretical values are close to experimental values from Ref. 3 (also shown in the figure for comparison) obtained from $[\text{Al}]=30\%$ structures.

The exciton binding energy E_X^{QWR} in a T -QWR is plotted in Figs. 3(b) and 3(c). Our results—12 meV for $x=0.3$ and

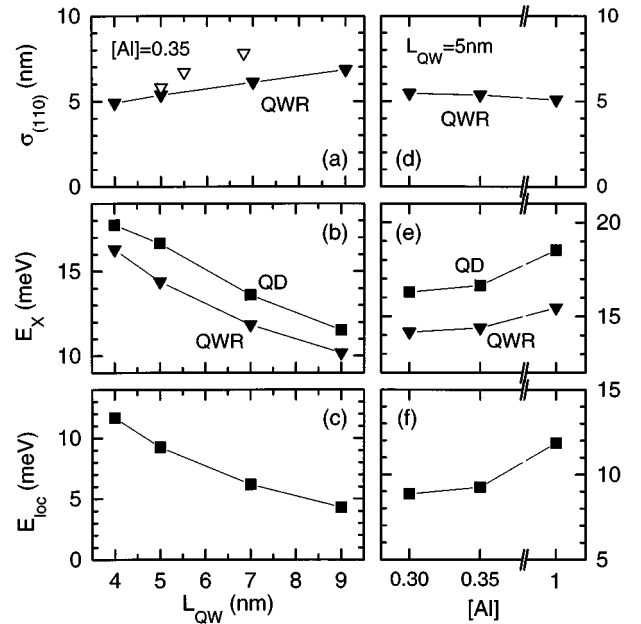


FIG. 3. (a) and (d) Extension of the exciton wave function in the (110) plane of a T -shaped quantum wire. (b) and (e) Exciton binding energy for CEO quantum wires and dots. (c) and (f) Localization energy for twofold CEO dots [see Eq. (2)]. The data are plotted in (a), (b), and (c) as a function of L_{QW} in the $\text{GaAs}/\text{Al}_{0.35}\text{Ga}_{0.65}\text{As}$ system. For (d), (e), and (f) the aluminum content in the barrier is varied for fixed $L_{\text{QW}}=5$ nm. Open triangles in (a) are experimental values for the exciton extension from Ref. 3.

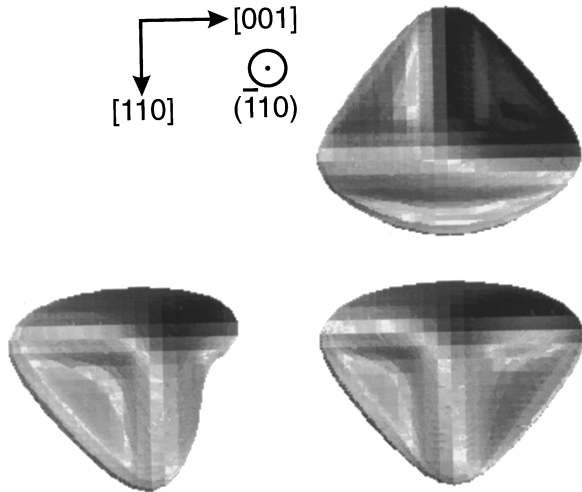


FIG. 4. Electron (excitonic) wave function (70% orbital) for a twofold CEO GaAs/Al_{0.35}Ga_{0.65}As quantum dot at the junction of three $L_{\text{QW}}=5$ nm quantum wells. The same orbital is shown from different angles.

15.5 meV for $x=1.0$ —are smaller than experimental results from Ref. 9, where 17 ± 3 meV for $x=0.3$ and 27 ± 3 meV for $x=1.0$ were found for L_{QW} close to 5 nm. Part of the discrepancy is due to image charge effects. If for AlAs barriers the barrier dielectric constant $\epsilon_r=10$ is used throughout the structure, we find $E_X^{\text{QWR}}=19$ meV. A further refinement could be obtained by treating the holes more accurately.

At the juncture of the three QWL planes, the electron and hole wave function become localized. In Fig. 4 the electron excitonic wave function is shown in different views. The extension of the wave function into the three quantum-well layers gives the orbital its characteristic shape. In Table II the wave-function extensions are listed for the single-particle

TABLE II. Extension of wave functions (in nm) for a twofold CEO GaAs/Al_{0.35}Ga_{0.65}As quantum dot with $L_{\text{QW}}=5$ nm.

	Ψ_e^0	Ψ_e^5	Ψ_h^0	Ψ_h^5
$\sigma_{[001]}$	6.6	4.9	5.5	3.0
$\sigma_{[110]}$	5.8	4.2	4.6	2.8
$\sigma_{[1\bar{1}0]}$	5.5	3.9	4.3	2.7

and excitonic wave functions. The Coulomb interaction leads to a general shrinking of the dot wave function, which also becomes more symmetric. Although the concept of exciton binding energy does not apply to quantum dots because the exciton cannot be dissociated within the dot, we use the term in the usual sense to compare the impact of Coulomb interaction in the different dimensions. We find [Fig. 3(b)] a further enhancement of exciton binding energy for the dot. The localization energy of the quantum dot E_{loc} is plotted in Fig. 3(c). A typical value of 10 meV makes the dot interesting for fundamental studies. Strong evaporation of carriers from QD's into connected QWR's is expected only at moderate temperatures ($T\geq 77$ K). Interesting transport and capture studies seem possible.

In conclusion, we predicted that twofold cleaved edge overgrowth leads to the formation of electronic quantum dots at the juncture of the three quantum-well planes. The localization energy of the exciton ground state with respect to the connected quantum wires can exceed 10 meV for the GaAs/Al_xGa_{1-x}As system. The exciton binding energy in the dot is enhanced with respect to the quantum wire. The spatially well-separated CEO quantum dots are expected to serve as an important structure for fundamental studies.

We acknowledge numerical support by O. Stier. This work has been funded by Deutsche Forschungsgemeinschaft in the framework of Sonderforschungsbereich 296.

*Electronic address: marius@sol.physik.tu-berlin.de
www: http://sol.physik.tu-berlin.de

¹L. N. Pfeiffer, K. W. West, H. L. Störmer, J. P. Eisenstein, K. W. Baldwin, D. Gershoni, and J. Spector, *Appl. Phys. Lett.* **56**, 1697 (1990).

²W. Wegscheider, L. N. Pfeiffer, M. M. Dignam, A. Pinczuk, K. W. West, S. L. McCall, and R. Hull, *Phys. Rev. Lett.* **71**, 4071 (1993).

³T. Someya, H. Akiyama, and H. Sakaki, *Phys. Rev. Lett.* **74**, 3664 (1995).

⁴M. Grundmann, O. Stier, and D. Bimberg, *Phys. Rev. B* **52**, 11 969 (1995); **50**, 14 187 (1994).

⁵*Semiconductors. Physics of Group IV Elements and III-V Compounds*, edited by O. Madelung, M. Schulz, and H. Weiss,

Landolt-Börnstein, New Series, Group III, Vol. 17, Pt. a (Springer, Berlin, 1982).

⁶L. Pfeiffer, H. Baranger, D. Gershoni, K. Smith, and W. Wegscheider, in *Low Dimensional Structures Prepared by Epitaxial Growth or Regrowth on Patterned Substrates*, edited by K. Eberl, P. M. Petroff, and P. Demester (Kluwer, Dordrecht, 1995), p. 93.

⁷D. B. Tran Thoai, R. Zimmermann, M. Grundmann, and D. Bimberg, *Phys. Rev. B* **42**, 5906 (1990).

⁸T. Someya, H. Akiyama, M. Yamauchi, H. Sugawara, H. Sakaki, *Solid-State Electron.* **40**, 315 (1996).

⁹T. Someya, H. Akiyama, and H. Sakaki, *Phys. Rev. Lett.* **76**, 2965 (1995).